



## Research article

# Defects oriented hydrothermal synthesis of TiO<sub>2</sub> and MnTiO<sub>2</sub> nanoparticles as photocatalysts for wastewater treatment and antibacterial applications

Ashir Mehmood Awan<sup>a</sup>, Awais Khalid<sup>b,\*</sup>, Pervaiz Ahmad<sup>b,c,\*\*</sup>, Abdulrahman I. Alharthi<sup>d</sup>, Muhammad Farooq<sup>a</sup>, Abdulhameed Khan<sup>e</sup>, Mayeen Uddin Khandaker<sup>f,g</sup>, Saad Aldawood<sup>h</sup>, Mshari A. Alotaibi<sup>d</sup>, Ahmed A. El-Mansi<sup>i</sup>, Mamdouh Basheir Eldesoqui<sup>j,k</sup>, Amal F. Dawood<sup>l</sup>, Samer H. Zyoued<sup>m,n</sup>

<sup>a</sup> Department of Physics, Hazara University Mansehra, Khyber Pakhtunkhwa, 21300, Pakistan

<sup>b</sup> Department of Physics, College of Science and Humanities, Prince Sattam Bin Abdulaziz University, P.O. Box 173, Al-Kharj, 11942, Saudi Arabia

<sup>c</sup> Department of Physics, University of Azad Jammu and Kashmir, Muzaffarabad, Pakistan

<sup>d</sup> Department of Chemistry, College of Science and Humanities, Prince Sattam Bin Abdulaziz University, P.O. Box 173, Al-Kharj, 11942, Saudi Arabia

<sup>e</sup> Department of Biotechnology, University of Azad Jammu and Kashmir, Muzaffarabad, 13100, Pakistan

<sup>f</sup> Applied Physics and Radiation Technologies Group, CCDCU, School of Engineering and Technology, Sunway University, Bandar Sunway, 47500, Selangor, Malaysia

<sup>g</sup> Faculty of Graduate Studies, Daffodil International University, Daffodil Smart City, Birulia, Savar, Dhaka, 1216, Bangladesh

<sup>h</sup> Department of Physics and Astronomy, College of Science, P.O. BOX 2455, King Saud University, Riyadh, 11451, Saudi Arabia

<sup>i</sup> Biology Department, Faculty of Science, King Khalid University, Abha, 61413, Saudi Arabia

<sup>j</sup> Department of Basic Medical Sciences, College of Medicine, AlMaarefa University, P.O. Box 71666, Riyadh, 11597, Saudi Arabia

<sup>k</sup> Department of Anatomy and Embryology, Faculty of Medicine, Mansoura University, P.O. Box 35516, Mansoura, Egypt

<sup>l</sup> Department of Basic Medical Sciences, College of Medicine, Princess Nourah Bint Abdulrahman University, P.O. Box 84428, Riyadh, 11671, Saudi Arabia

<sup>m</sup> Department of Mathematics and Sciences, Ajman University, P.O. Box 346, Ajman, United Arab Emirates

<sup>n</sup> Center of Medical and Bio-Allied Health Sciences Research, Ajman University, P.O. Box 346, Ajman, United Arab Emirates

## ARTICLE INFO

## Keywords:

TiO<sub>2</sub>  
MnTiO<sub>2</sub>-NPs  
Nanoparticles  
Antibacterial  
Photocatalyst  
Photodegradation

## ABSTRACT

Pure and manganese-doped titanium dioxide nanoparticles (MnTiO<sub>2</sub>-NPs) were synthesized by the defect-oriented hydrothermal approach. The synthesized material was then characterized by X-ray diffraction (XRD), Scanning electron microscopy (SEM), Energy dispersive X-ray spectroscopy (EDX), and UV-visible spectroscopy (UV-Vis). The agar well diffusion method assessed the antibacterial efficiency of TiO<sub>2</sub> and MnTiO<sub>2</sub>-NPs against *E. coli* and *S. aureus*. Zone of inhibition (ZOI) formed by pure TiO<sub>2</sub> was observed as 12 mm and 11.5 mm against *E. coli* and *S. aureus*, while for MnTiO<sub>2</sub>-NPs it was observed as 19 mm (*E. coli*) and 21 mm (*S. aureus*). The concentration of synthesized nanoparticles (10 mg/ml, and 20 mg/ml) was used for antibacterial studies. The efficacy of the pure and MnTiO<sub>2</sub>-NPs as an active photocatalyst for the degradation of methylene blue (MB) dye was also assessed using a UV light. It was observed that the

\* Corresponding author. Department of Physics, College of Science and Humanities, Prince Sattam Bin Abdulaziz University, P.O. Box 173, Al-Kharj, 11942, Saudi Arabia.

\*\* Corresponding author. Department of Physics, College of Science and Humanities, Prince Sattam Bin Abdulaziz University, P.O. Box 173, Al-Kharj, 11942, Saudi Arabia.

E-mail addresses: [ak.khalid@psau.edu.sa](mailto:ak.khalid@psau.edu.sa) (A. Khalid), [pervaiz.pas@yahoo.com](mailto:pervaiz.pas@yahoo.com) (P. Ahmad).

<https://doi.org/10.1016/j.heliyon.2024.e25579>

Received 2 November 2023; Received in revised form 26 January 2024; Accepted 30 January 2024

Available online 4 February 2024

2405-8440/© 2024 The Authors. Published by Elsevier Ltd. This is an open access article under the CC BY-NC-ND license (<http://creativecommons.org/licenses/by-nc-nd/4.0/>).

photodegradation efficiency of 1 g of MnTiO<sub>2</sub>-NPs was higher than the same amount of pure TiO<sub>2</sub>. The results suggest that the photocatalyst concentration directly impacts the photodegradation of MB dye. The pH value was found to influence the photodegradation of MB dye at higher pH values. Based on the obtained results, MnTiO<sub>2</sub>-NPs were observed as a promising agent for microbial resistance and water remediation.

## 1. Introduction

Titanium dioxide (TiO<sub>2</sub>) is a semiconductor material with a tetragonal crystal structure and a bandgap of 3.2 eV in its pure form. The characteristics of nanomaterials are improved due to the intensification of broken bonds on the surface and surface to volume ratio of the nanoparticles [1]. The surface of nanostructured materials has broken bonds that significantly modify the surface energy, which in turn tunes the band gap of the material. This can lead to changes in the crystalline structure of the material. Recent studies have shown that the optical bandgap of the nanomaterials varies with particle size. This variation in bandgap results in changes in the optical and electrical properties of the nanoparticles, making them suitable for a variety of applications [2,3]. The performance of nanomaterials is also affected by their size and morphology, which are influenced by their high surface-to-volume ratio. The properties including optical, electrical, thermal, photocatalytic, antibacterial, and gas sensing can be enhanced by incorporating various types of nanomaterials. The most commonly used nanomaterials for photocatalysis and antibacterial applications are Fe<sub>2</sub>O<sub>3</sub>, CuO, Co<sub>3</sub>O<sub>4</sub>, Ag<sub>2</sub>O, ZnO, BN, CeO<sub>2</sub>, and TiO<sub>2</sub> [4–12].

TiO<sub>2</sub> has three natural polymorphs: anatase, rutile, and brookite [13,14]. TiO<sub>2</sub> is a prominent photocatalytic material that has been extensively used in various applications such as air and water purification, treating various microbial diseases, and self-cleaning surfaces [15]. TiO<sub>2</sub> does not effectively absorb the solar light. The optical absorption of TiO<sub>2</sub> is limited to the UV region due to its wide bandgap, which results in low photocatalytic activity under visible light irradiation [16–18]. It is believed that the photocatalytic activity of TiO<sub>2</sub> can be significantly enhanced by depositing or doping suitable semiconductor metal oxides, noble metals, transition metal ions, or nonmetal ions into or onto the TiO<sub>2</sub> structure [19,20]. Various strategies have been developed to modify the TiO<sub>2</sub> properties and to address its limitations, including doping with transition metal ions [21]. One of the transition metal ions that has been successfully used for doping is manganese (Mn), which is known to enhance the photocatalytic activity of TiO<sub>2</sub> by shifting its absorption spectrum toward the visible light region. MnTiO<sub>2</sub>-NPs have been reported to exhibit visible light absorption, making them attractive photocatalysts for visible light-driven applications. The incorporation of Mn ions into the TiO<sub>2</sub> lattice alters the band structure of TiO<sub>2</sub>, leading to the creation of mid-gap states that promote visible light absorption.

TiO<sub>2</sub> and MnTiO<sub>2</sub>-NPs have been extensively studied for their antibacterial properties. The photocatalytic activity of TiO<sub>2</sub> can generate reactive oxygen species (ROS), which are toxic to bacteria [22–25]. The ROS can damage bacterial cell membranes, leading to bacterial death. TiO<sub>2</sub> and MnTiO<sub>2</sub>-NPs are effective against various bacteria, including *Escherichia coli*, *Staphylococcus aureus*, and *Pseudomonas aeruginosa*. MnTiO<sub>2</sub>-NPs have been reported to exhibit higher antibacterial activity than pure TiO<sub>2</sub> due to its enhanced visible light absorption. The photocatalytic degradation of organic dyes is another important application of TiO<sub>2</sub> and MnTiO<sub>2</sub>-NPs. Organic dyes are widely used in various industries, including textile, paper, and leather. The discharge of dye-containing wastewater can cause environmental pollution and health hazards. TiO<sub>2</sub> and MnTiO<sub>2</sub>-NPs can effectively degrade organic dyes under UV and visible light irradiation. The degradation mechanism involves the generation of ROS, which can break down the organic dye molecules into smaller and less harmful molecules. MnTiO<sub>2</sub>-NPs have been reported to exhibit higher photocatalytic activity than pure TiO<sub>2</sub> due to its enhanced visible light absorption. S. Ragupathy et al. synthesized Mn-doped SnO<sub>2</sub> which appears to be a promising photocatalyst for visible light-driven degradation of organic pollutants like brilliant green. Its impressive 92.84 % degradation efficiency in visible light stems from its lower band gap (3.57 eV) and larger surface area (32.70 m<sup>2</sup>/g) improves light absorption and minimizes charge carrier recombination [26,27].

Hydrothermal synthesis is a versatile and cost-effective method for producing TiO<sub>2</sub> and MnTiO<sub>2</sub>-NPs with tuneable properties. The size, shape, and crystalline structure of the nanoparticles can be controlled by adjusting the reaction conditions, such as the temperature, pressure, and pH of the solution. Hydrothermal synthesis has several advantages over other methods of producing TiO<sub>2</sub> and MnTiO<sub>2</sub>-NPs. It is a relatively simple and safe process that does not require the use of toxic chemicals. It is also a scalable process, which means that it can be used to produce large quantities of nanoparticles. Additionally, hydrothermal synthesis can be used to produce nanoparticles with a high degree of purity and uniformity [28].

Unlike previous studies where porous and complex structures of MnTiO<sub>2</sub> were produced by hydrothermal thermal technique in a growth duration of 3.33 h with a dye degradation efficiency of 75 % for methylene blue [29], we introduced a simple defects-oriented hydrothermal technique for the synthesis of MnTiO<sub>2</sub> nanoparticles in a comparative short growth duration of 1.6 h and enhanced dye degradation efficiency for methylene blue and excellent antibacterial activities for different gram-positive and gram-negative bacteria.

## 2. Material and methods

### 2.1. Materials

TiO<sub>2</sub> (bulk), and MnCl<sub>2</sub> were used as precursors, while sodium hydroxide (NaOH) was used as a reducing agent. These were procured from Sigma Aldrich, St. Louis, MO, USA. Reagents (99 % analytically graded) were used as received without further

refinement. The synthesized material was analyzed by a scanning electron microscope (SEM: JEOL 7000F), Energy-dispersive X-ray spectroscopy (EDX), Siemens D5000 X-ray diffractometer, and UV-visible-NIR spectrophotometer (Model-V770, JASCO) was used to study various features of the prepared material.

## 2.2. Preparation of TiO<sub>2</sub>

TiO<sub>2</sub> and MnTiO<sub>2</sub>-NPs were synthesized by the hydrothermal method. TiO<sub>2</sub> (bulk), and MnCl<sub>2</sub> were used as precursors, while sodium hydroxide (NaOH) was used as a reducing agent. For the pure TiO<sub>2</sub> sample, initially, 5 g of TiO<sub>2</sub> was taken in 70 ml of deionized water in a beaker under continuous stirring to get a homogenous mixture. The pH of the solution was adjusted to 9 by adding NaOH (1.25 M) and continuously stirred for 30 min. The same procedure was followed to prepare MnTiO<sub>2</sub>-NPs by adding MnCl<sub>2</sub> (0.5 g) along with TiO<sub>2</sub> (bulk). The reactant mixture of light brown color was shifted to an autoclave and placed in an oven at 180 °C for 18 h. After equating to room temperature automatically, the resulting product was obtained using centrifugation and washed out with deionized water in addition to ethanol, then dried at 90 °C for 2 h.

## 2.3. Antibacterial assay

The antibacterial activity of pure TiO<sub>2</sub> and MnTiO<sub>2</sub>-NPs was evaluated against clinical isolates of gram-positive and gram-negative bacteria. Two different bacterial species were selected for antibacterial screening in the current study: *Escherichia coli* isolated from clinical specimens of urinary tract infections (UTI) as gram-negative bacteria while *Staphylococcus aureus* (UTI) as gram-positive bacteria. The agar well diffusion method was used accordingly to measure the zone of inhibition (ZOI) of bacterial growth after treatment with different doses (10 mg/ml, and 20 mg/ml) of the nanoparticles dissolved in DMSO [30]. To culture, turbidity adjustments, and incubation same parameters were followed [9] and Each experiment was repeated thrice (N = 3).

## 2.4. Photocatalytic activity

The photocatalytic activity of TiO<sub>2</sub> and MnTiO<sub>2</sub>-NPs was evaluated through the photodegradation of methylene blue (MB) under UV irradiation. To conduct the photocatalytic activity a UV light source (US-800 (250W)), and a Pyrex beaker were used. 0.1 g of TiO<sub>2</sub> and MnTiO<sub>2</sub>-NPs as a catalyst was poured separately in 50 ml of 10 mg/L (10 ppm) solution of MB dye. For the degradation process, the solution was exposed to UV light on a rotary shaker (100 rpm) for predetermined intervals up to 100 min at room temperature. MB Degradation is calculated with the help of the following formula:

$$\text{MB Degradation (\%)} = (A_0 - A_t) / A_0 \times 100 \quad (1)$$

Where  $A_t$  is the absorbance of the MB solution after  $t$  hours of exposure to the UV source and  $A_0$  is the starting absorbance of the MB solution.

## 2.5. Characterization

The synthesized powder form of the synthesized sample was characterized by a scanning electron microscope (SEM: JEOL 7000F) to check its apparent shape and morphology. Energy-dispersive X-ray spectroscopy (EDX) is used in conjunction with SEM to provide

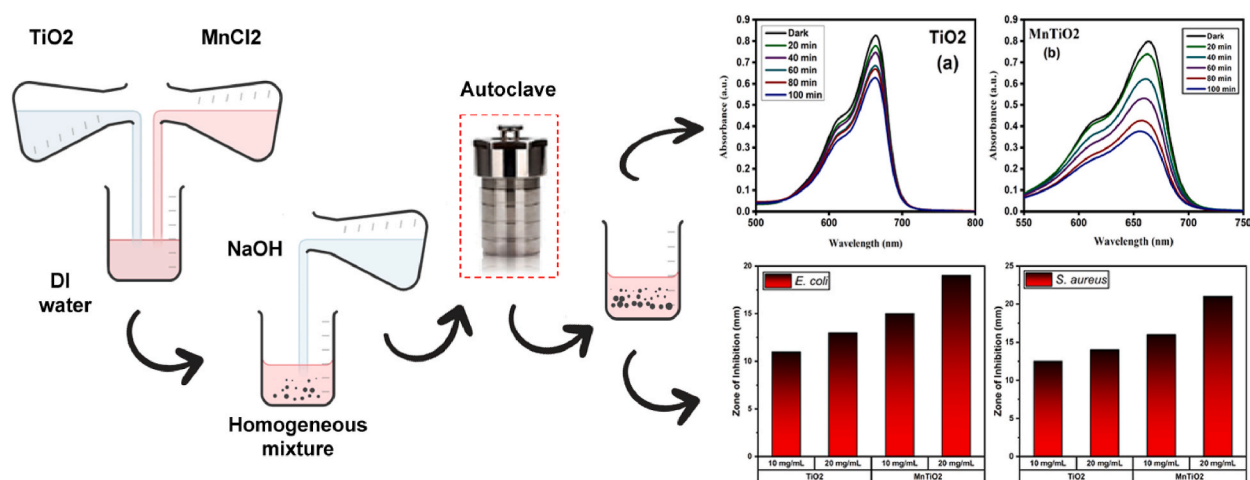


**Fig. 1.** A summary of the complete methodology from the hydrothermal synthesis of MnTiO<sub>2</sub>-NPs to its antibacterial activity and photocatalytic dye degradation.

elemental information on the surface of the synthesized material. The crystal structure of the samples was measured by a Siemens D5000 X-ray diffractometer by using Cu K $\alpha$  radiation with an operating voltage of 20 kV and an angle of incidence of 3° in all cases. The UV–visible–NIR spectrophotometer (Model-V770, JASCO) was used to study the optical properties of the material. The complete summary of methodology from synthesis, characterization, antibacterial activity, and photodegradation of methylene blue of TiO<sub>2</sub> and MnTiO<sub>2</sub>-NPs is shown via a sketch in Fig. 1.

### 3. Results and discussion

#### 3.1. XRD analysis

The X-ray powder diffraction (XRD) technique was used to analyze the crystalline structure of pure and MnTiO<sub>2</sub>-NPs synthesized by the hydrothermal technique. The XRD pattern of the samples is shown in Fig. 2. The 2 $\theta$  peaks at 25.32°, 37.79°, 48.06°, 53.90°, 55.083°, 62.66°, 69.40°, 70.32°, and 75.06° corresponds to the crystal planes of all samples at (101), (004), (200), (105), (211), (204), (116), (220), and (215), respectively. The XRD results reveal that all the samples exhibit the anatase phase with (JCPDS Card No. 78–2486) [31]. The sharpness of peaks shows the crystalline nature of the synthesized material whereas the broadening of peaks indicates the reduction in size of the crystalline material, calculated by using the Modified-Scherer formula. The average crystalline size of the base and doped samples was 36 nm and 34 nm, respectively. The grain size (D) for all samples was determined from the full width at half maximum (FWHM) and was in the range of 34–36 nm. The crystallinity of the TiO<sub>2</sub> and MnTiO<sub>2</sub>-NPs was 64.9 % and 66.5 %, respectively.

#### 3.2. SEM analysis

The surface morphology and shape of the samples were analyzed by SEM. The SEM micrographs of pure TiO<sub>2</sub> in lower and higher magnifications are shown in Fig. 3 (a), and (b) whereas that of MnTiO<sub>2</sub>-NPs samples are displayed in Fig. 3 (c), and (d). The nanoparticles exhibited an almost spherical shape, and their average diameter varied with the concentration of Mn [32].

The histograms of each type of synthesized nanoparticles are shown in Fig. 4 (a, b). The particle size of the synthesized nanomaterial is shown on the horizontal axis of the histogram whereas the frequency (Count of nanoparticles) regarding each size range is shown on the vertical axis of the histogram. The height of the vertical bars shows the number of particles in each size range. According to the histogram, the average diameter of the base sample was 68 nm, as shown in Fig. 4 (a), whereas, for doped samples with Mn, the average diameter was about 46 nm, as shown in Fig. 4 (b).

#### 3.3. EDX analysis

The elemental composition of pure and MnTiO<sub>2</sub>-NPs was confirmed through EDX analysis. The EDX results for pure TiO<sub>2</sub>, and MnTiO<sub>2</sub>-NPs, are shown in Fig. 5(a), and Fig. 5(b) respectively. Only Ti and O peaks appeared in Fig. 5(a), while Ti, O, and Mn peaks were observed in Fig. 5(b), indicating the successful incorporation of Mn in TiO<sub>2</sub> [33]. EDX spectra confirm that no extra peaks are observed. The elemental composition by weight % and atomic % observed in TiO<sub>2</sub> and MnTiO<sub>2</sub>-NPs in the EDX analysis is shown in Table 1.

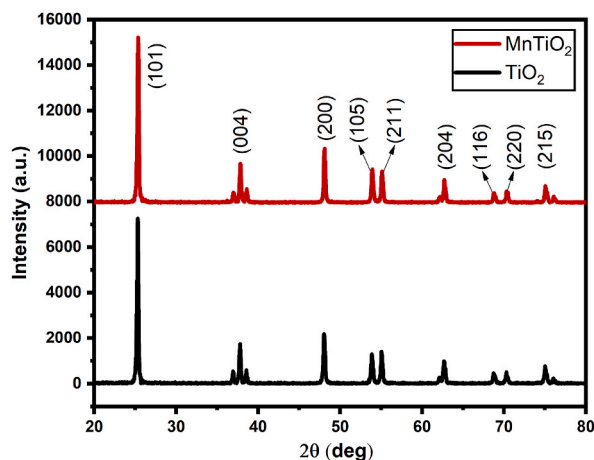
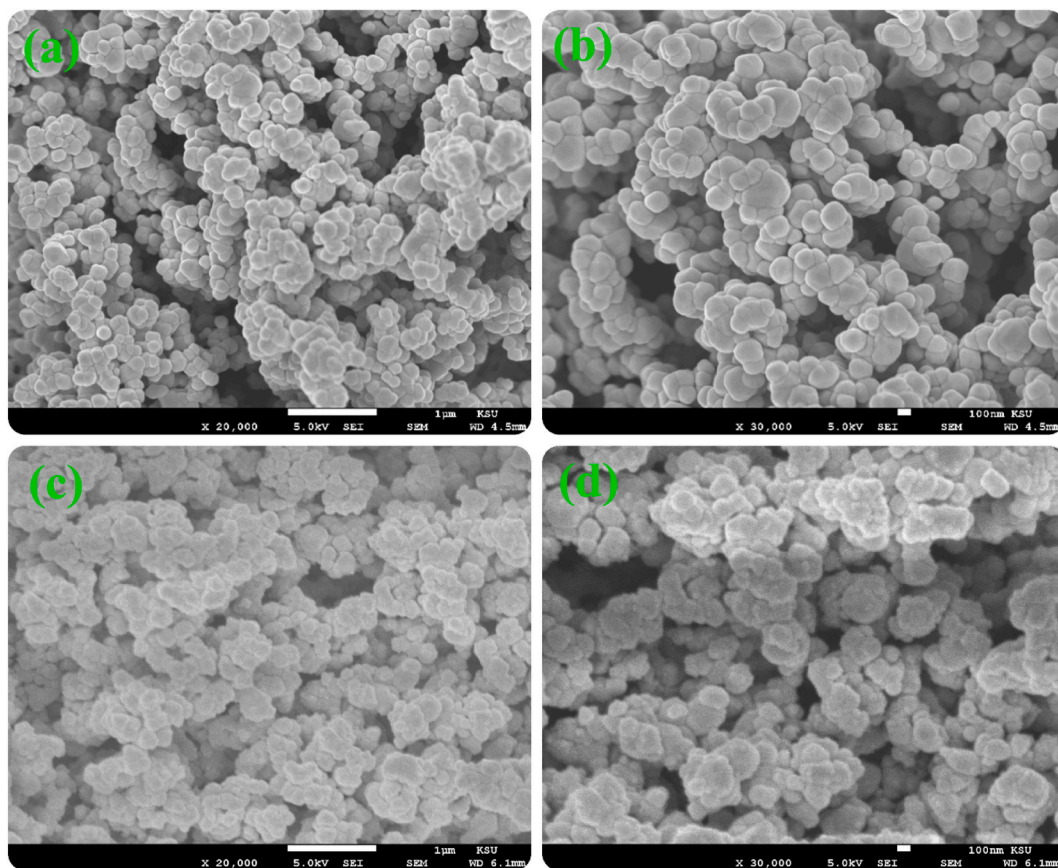
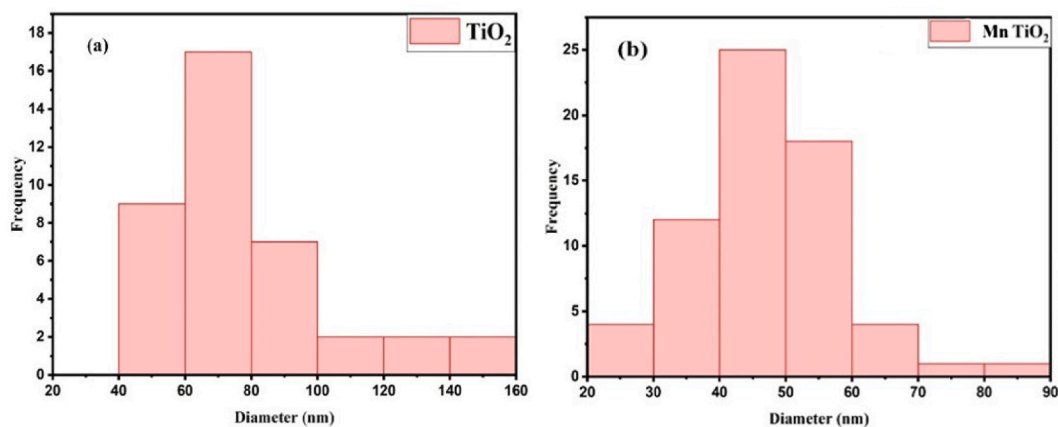


Fig. 2. XRD pattern of TiO<sub>2</sub> (plotted in black), and MnTiO<sub>2</sub>-NPs (plotted in red). (For interpretation of the references to color in this figure legend, the reader is referred to the Web version of this article.)



**Fig. 3.** (a) Lower, and (b) higher magnification SEM micrographs of pure  $\text{TiO}_2$ . (c) Lower, and (d) higher magnification SEM micrographs of  $\text{MnTiO}_2$ -NPs.



**Fig. 4.** Histogram of (a) pure and (b)  $\text{Mn-TiO}_2$  (5 %, 10 %) NPs.

### 3.4. UV-vis spectroscopy

The UV-Vis absorption spectra of pure and  $\text{MnTiO}_2$ -NPs are shown in Fig. 6. The band gap was calculated by Tauc plot relation. The calculated band gaps from the Tauc plot relation for pure and  $\text{MnTiO}_2$ -NPs were 2.70, and 2.61 eV, respectively, indicating that Mn doping minimizes the energy gap. Anatase's band gap value was lower than the experimentally measured value of 3.2 eV, apparently as a result of surface scattering-induced optical trapping [34].

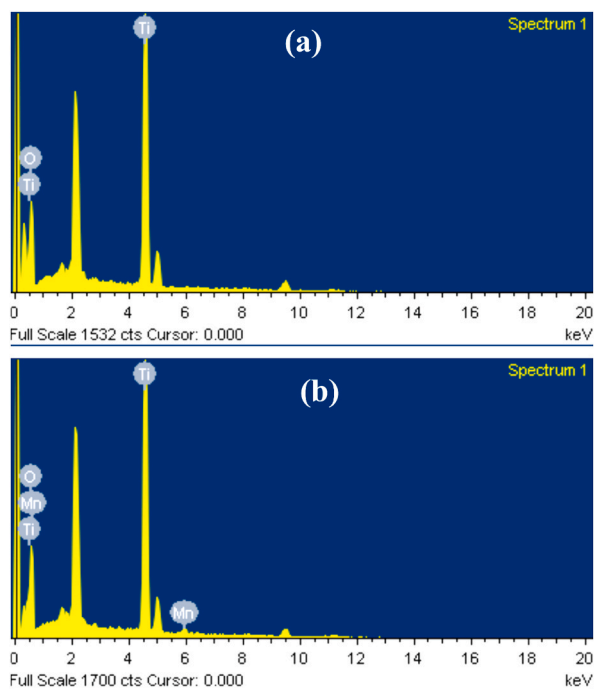


Fig. 5. EDX results for (a) pure  $\text{TiO}_2$ , and (b)  $\text{MnTiO}_2$ -NPs.

Table 1

Elemental composition by weight and atomic% observed in  $\text{TiO}_2$  and  $\text{MnTiO}_2$ -NPs.

Element	$\text{TiO}_2$		$\text{Mn-TiO}_2$	
	Weight%	Atomic%	Weight%	Atomic%
O K	41.51	68.00	39.86	66.59
Ti K	58.49	32.00	58.17	32.46
Mn K			1.96	0.96
Totals	100.00		100.00	

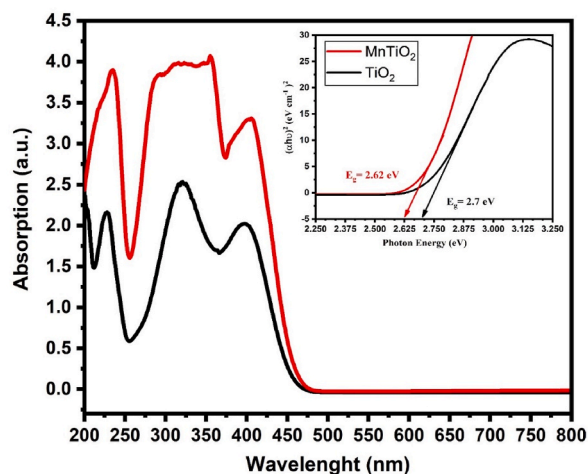


Fig. 6. The absorption spectra and band gap for  $\text{TiO}_2$  and  $\text{MnTiO}_2$ -NPs.

### 3.5. Antibacterial activities

The antibacterial activity of pure TiO<sub>2</sub> and MnTiO<sub>2</sub>-NPs was evaluated against clinical isolates of gram-positive (*S. aureus*) and gram-negative (*E. coli*) bacteria obtained from Combined Military Hospital (CMH) Muzaffarabad. The agar well diffusion method was used to measure the zone of inhibition (ZOI) of bacterial growth after treatment with different doses (10 mg, and 20 mg/ml) of the nanoparticles dissolved in DMSO.

The results indicated that both pure TiO<sub>2</sub> and MnTiO<sub>2</sub>-NPs exhibited antibacterial activity against *S. aureus* and *E. coli* as shown in Fig. 7. However, MnTiO<sub>2</sub>-NPs showed better antibacterial activity compared to pure TiO<sub>2</sub>-NPs [35]. The ZOI values of MnTiO<sub>2</sub>-NPs were higher than those of pure TiO<sub>2</sub> for both *S. aureus* and *E. coli* at all tested doses. The difference in antibacterial activity between pure and MnTiO<sub>2</sub>-NPs can be attributed to the structural differences between gram-positive and gram-negative bacteria, as well as the increase in doping concentration of manganese. Fig. 8 shows petri plates used to analyze the efficiency of synthesized nanomaterials while Table 2 shows observed ZOI (mm) for Base and MnTiO<sub>2</sub>-NPs against different bacteria.

Previous studies have reported that MnTiO<sub>2</sub>-NPs exhibit better antibacterial activity than pure TiO<sub>2</sub> nanoparticles [36]. According to our results, it is because of the Mn-doping which introduced defects in the crystal lattice of TiO<sub>2</sub>, which enhanced the photocatalytic and antibacterial activities of the nanoparticles. The presence of Mn also increases the surface area and alters the surface charge of the nanoparticles, which can further enhance their antibacterial activity.

It can be observed that MnTiO<sub>2</sub>-NPs have better antibacterial activity against both gram-positive and gram-negative bacteria compared to pure TiO<sub>2</sub> nanoparticles. These findings suggest that MnTiO<sub>2</sub>-NPs have potential applications in the development of antibacterial agents for various biomedical and environmental applications.

### 3.6. Photocatalytic activity

The photocatalytic activity of TiO<sub>2</sub> and MnTiO<sub>2</sub>-NPs was evaluated through the photodegradation of methylene blue (MB) under UV irradiation. The photocatalytic activity was evaluated by measuring the absorbance of the MB solution at different time intervals.

The results displayed in Fig. 9 (a), and (b) showed that both pure TiO<sub>2</sub> and MnTiO<sub>2</sub>-NPs exhibited photocatalytic activity, and the degradation rate was enhanced upon doping with Mn. The degradation of MB was found to be dependent on the concentration of the nanoparticles and the doping concentration of Mn [31,37].

Fig. 9 shows that the highest degradation rate was observed with MnTiO<sub>2</sub>-NPs, which degraded 78 % of MB after 100 min of irradiation, while pure TiO<sub>2</sub> nanoparticles degraded 51 % of MB under the same conditions.

The enhanced photocatalytic activity of MnTiO<sub>2</sub>-NPs can be attributed to several factors. Firstly, Mn doping modifies the crystal structure and bandgap of TiO<sub>2</sub>, which enhances the absorption of UV light and increases the generation of reactive oxygen species (ROS). ROS plays a crucial role in the degradation of organic pollutants by attacking the organic molecules and breaking them down into smaller, less harmful molecules [38]. Secondly, Mn doping increases the surface area and pore volume of TiO<sub>2</sub> nanoparticles, which enhances the adsorption of MB onto the surface of nanoparticles, leading to an increase in the efficiency of photocatalytic degradation [39].

This study also thoroughly investigated the impact of various experimental conditions such as time, initial dye concentration, amount of catalyst, and pH. Fig. 10 (a) demonstrates a time vs degradation graph, in which direct variation is observed. The rate of degradation is higher for MnTiO<sub>2</sub> than for pure TiO<sub>2</sub>. An increase in time duration results in a corresponding increase in the percent photodegradation of MB. Furthermore, Fig. 10 (b) showed that the concentration of photocatalyst has a direct influence on the photodegradation of MB dye, as increasing its concentration (0.1 g, 0.25 g, 0.5 g, and 0.75 g) led to an increase in photodegradation. The rate of degradation of MnTiO<sub>2</sub> is higher than TiO<sub>2</sub>. Similarly, Fig. 10 (c) demonstrated that the photodegradation of MB was reduced due to an increase in the concentration of dye with the photocatalyst. The efficiency of MnTiO<sub>2</sub> was reduced more by

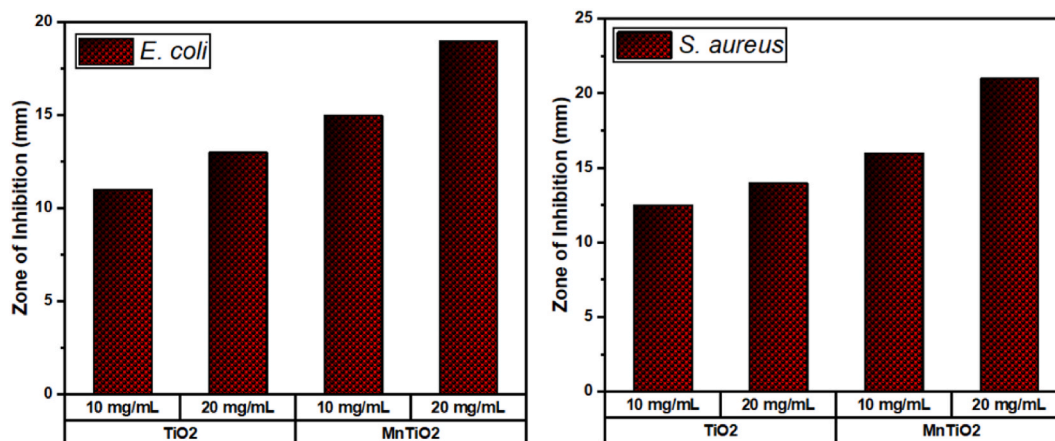


Fig. 7. Bar graph shows the variation for both nanomaterials against tested microbes.

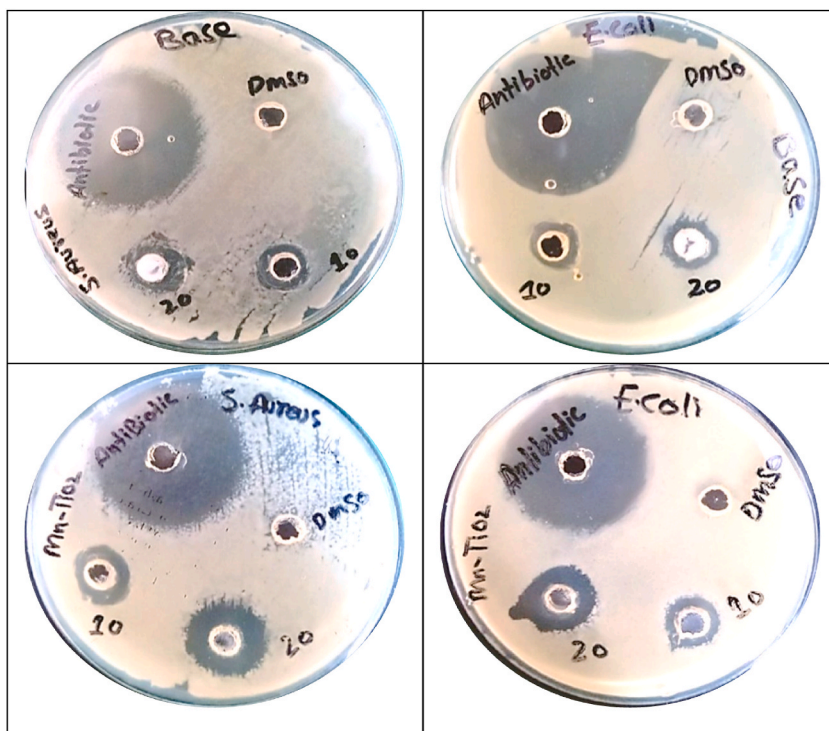


Fig. 8. Antibacterial activity of  $TiO_2$  and  $MnTiO_2$ -NPs.

Table 2  
ZOI (mm) of pure and  $MnTiO_2$ -NPs against different bacteria.

Samples	Concentration (mg/ml)	Zone of inhibition (mm)	
		E. Coli	S. Aureus
$TiO_2$	10 mg/ml	11 mm	12.5 mm
	20 mg/ml	13 mm	14 mm
10 % $Mn-TiO_2$	10 mg/ml	15 mm	16 mm
	20 mg/ml	19 mm	21 mm

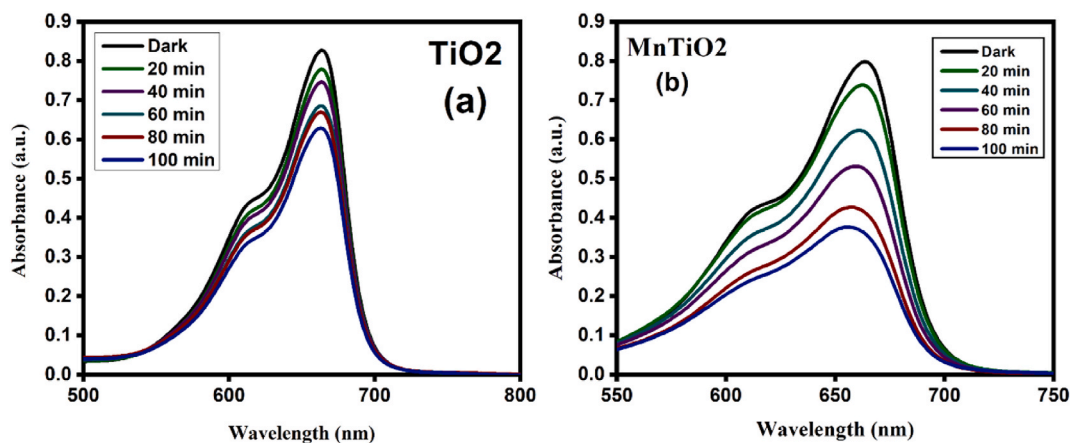
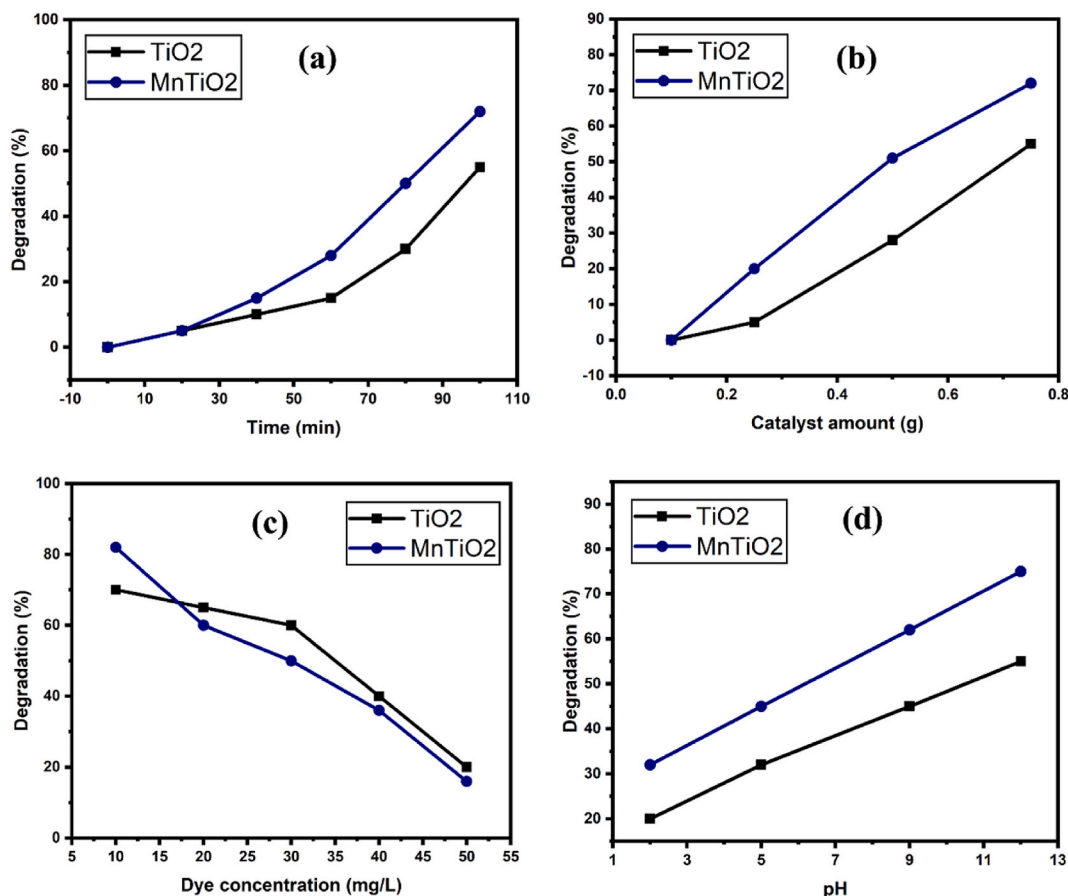


Fig. 9. Absorbance spectra of (a)  $TiO_2$ , and (b)  $MnTiO_2$  samples.



**Fig. 10.** (a) Demonstrates the time vs degradation graph, (b) shows that the concentration of photocatalyst has a direct influence on the photodegradation of MB dye, (c) demonstrates that photodegradation of MB reduced due to an increase in the concentration of dye with the photocatalyst. (d) The pH level was found to impact the photodegradation of MB.

increasing MB concentration than pure TiO<sub>2</sub>. MnTiO<sub>2</sub> has a narrower bandgap than TiO<sub>2</sub>, which means that it absorbs light with low energy. MnTiO<sub>2</sub> is less likely to be excited and generate hydroxyl radicals, which are the primary requirement for photocatalysis. Finally, from Fig. 10 (d), the pH level was found to impact the photodegradation of MB, with higher pH (2, 5, 9, 12) values resulting in greater photodegradation when using MnTiO<sub>2</sub> as a catalyst. These findings highlight the importance of doping to enhance the efficiency of the materials. Additionally, MnTiO<sub>2</sub>-NPs exhibited better stability and reusability than pure TiO<sub>2</sub> nanoparticles, making them promising candidates for practical applications in wastewater treatment.

#### 4. Conclusion

This study unveils a novel, rapid hydrothermal technique successfully employed to synthesize MnTiO<sub>2</sub> nanoparticles (MnTiO<sub>2</sub>-NPs) exhibiting remarkable antibacterial and photocatalytic properties. Compared to conventional methods, this approach significantly reduces growth duration while introducing desirable defect sites within the material. The synthesized MnTiO<sub>2</sub>-NPs exhibit an anatase phase, a crystalline structure, and an average particle size in the 34–36 nm range. The EDX analysis confirms the successful doping of Mn into the sample, while UV–Vis analysis data indicates a reduction in band gap upon doping Mn into TiO<sub>2</sub>, demonstrating the creation of defect sites responsible for enhanced photocatalytic and antibacterial activity. The photocatalytic activity evaluation reveals that MnTiO<sub>2</sub>-NPs exhibit significantly greater photocatalytic activity than pure TiO<sub>2</sub>. The antibacterial activity was also tested against *E. coli* and *S. aureus*, MnTiO<sub>2</sub>-NPs shows superior antibacterial efficacy than pure TiO<sub>2</sub>. By optimizing the synthesis process and delving deeper into the mechanism of action, we envision these engineered MnTiO<sub>2</sub>-NPs as next-generation materials with multifaceted applications benefiting various sectors including energy, biomedical, and environment.

#### Data availability statement

All the relevant data is available in the manuscript.

## Funding

This research was funded by Princess Nourah bint Abdulrahman University Researchers Supporting Project number (PNURSP2023R110), Princess Nourah bint Abdulrahman University, Riyadh, Saudi Arabia.

## CRediT authorship contribution statement

**Ashir Mehmood Awan:** Writing – review & editing, Writing – original draft, Visualization, Validation, Methodology, Investigation, Formal analysis, Data curation, Conceptualization. **Awais Khalid:** Writing – review & editing, Writing – original draft, Validation, Resources, Methodology, Investigation, Formal analysis, Data curation, Conceptualization. **Pervaiz Ahmad:** Writing – review & editing, Writing – original draft, Validation, Supervision, Resources, Project administration, Methodology, Funding acquisition, Formal analysis, Data curation, Conceptualization. **Abdulrahman I. Alharthi:** Writing – review & editing, Resources, Methodology, Investigation, Formal analysis, Data curation, Conceptualization. **Muhammad Farooq:** Writing – review & editing, Visualization, Validation, Supervision, Investigation, Data curation, Conceptualization. **Abdulhameed Khan:** Writing – review & editing, Validation, Software, Resources, Methodology, Formal analysis, Data curation, Conceptualization. **Mayeen Uddin Khandaker:** Writing – review & editing, Validation, Supervision, Software, Resources, Project administration, Funding acquisition, Formal analysis, Data curation, Conceptualization. **Saad Aldawood:** Writing – review & editing, Visualization, Resources, Methodology, Investigation, Data curation. **Mshari A. Alotaibi:** Writing – review & editing, Validation, Software, Resources, Investigation, Formal analysis. **Ahmed A. El-Mansi:** Writing – review & editing, Visualization, Software, Resources, Funding acquisition. **Mamdouh Basheir Eldesoqui:** Visualization, Validation, Software, Resources. **Amal F. Dawood:** Visualization, Software, Investigation, Conceptualization. **Samer H. Zyoud:** Validation, Resources, Investigation, Funding acquisition, Formal analysis.

## Declaration of competing interest

The authors declare that they have no known competing financial interests or personal relationships that could have appeared to influence the work reported in this paper.

The author is an Editorial Board Member/Editor-in-Chief/Associate Editor/Guest Editor for [*Journal name*] and was not involved in the editorial review or the decision to publish this article.

The authors declare the following financial interests/personal relationships which may be considered as potential competing interests.

## Acknowledgment

The authors extend their appreciation to the Deanship of Scientific Research at King Khalid University for funding this work through a large group research project under a grant number (R.G.P.2/66/44).

## References

- [1] Z.V. Saponjic, N.M. Dimitrijevic, O.G. Poluektov, L.X. Chen, E. Wasinger, U. Welp, D.M. Tiede, X. Zuo, T.J.T.J.o.P.C.B. Rajh, Charge separation and surface reconstruction: a Mn<sup>2+</sup> doping study, *J. Phys. Chem. B* 110 (2006) 25441–25450.
- [2] E. Gazo-Hanna, A. Poitou, P. Casari, L. Juras, Study of interply slip during thermoforming of continuous fiber composite materials, in: *Proceedings of The 18th International Conference on Composite Materials (ICCM-18)*, Jeju Island, Korea, 2011.
- [3] E.G. Hanna, A. Poitou, P.J.M.P. Casari, Mechanics, Modeling the interply slip during forming of thermoplastic laminates, *Mater. Phys. Mech.* 40 (2018) 22–36.
- [4] M.I. Irshad, P. Ahmad, A. Khalid, M.M. Alam, N. Sobahi, I.U. Din, R. Nazir, A.I. Alharthi, F. Rehman, A. Yar, Evaluation of structural, magnetic and concentration dependent texture variations of electrodeposited cobalt nanowires, *Mater. Sci. Semicond. Process.* 152 (2022) 107042.
- [5] I.A. Ahmed, H.S. Hussein, Z.A. Alotman, A.G. Alanazi, N.S. Alsaari, A. Khalid, Green synthesis of Fe–Cu bimetallic supported on alginate-limestone nanocomposite for the removal of drugs from contaminated water, *Polymers* 15 (2023) 1221.
- [6] R.A. Basit, Z. Abbasi, M. Hafeez, P. Ahmad, J. Khan, M.U. Khandaker, K.S. Al-Mugren, A. Khalid, Successive photocatalytic degradation of methylene blue by ZnO, CuO and ZnO/CuO synthesized from coriandrum sativum plant extract via green synthesis technique, *Crystals* 13 (2023) 281.
- [7] S. Shakeel, F.N. Talpur, Sirajuddin, N. Anwar, M.A. Iqbal, A. Ibrahim, H.I. Afridi, A. Unar, A. Khalid, I.A. Ahmed, Xanthan gum-mediated silver nanoparticles for ultrasensitive electrochemical detection of Hg<sup>2+</sup> ions from water, *Catalysts* 13 (2023) 208.
- [8] A. Hyder, M. Thebo, D. Janwery, J.A. Buledi, I. Chandio, A. Khalid, B.S. Al-Anzi, H.A. Almukhlifi, K.H. Thebo, F.N. Memon, Fabrication of Para-Dimethylamine Calix [4] Arene Functionalized Self-Assembled Graphene Oxide Composite Material for Effective Removal of 2, 4, 6-Tri-Chlorophenol from Aqueous Environment, *Heliyon*, 2023.
- [9] A. Jabeen, A. Khan, P. Ahmad, A. Khalid, Z. Majeed, Z. Anjum, Y. Modafar, O.A. Jefri, A.M. Alanazi, A.M. Saeedi, Biomedical and photocatalytic dye degradation studies of Cymbopogon citratus mediated copper oxide nanoparticles (CuO NPs), *J. Drug Deliv. Sci. Technol.* (2023) 104795.
- [10] S. Habib, F. Rashid, H. Tahir, I. Liaqat, A.A. Latif, S. Naseem, A. Khalid, N. Haider, U. Hani, R.A. Dawoud, Antibacterial and cytotoxic effects of biosynthesized zinc oxide and titanium dioxide nanoparticles, *Microorganisms* 11 (2023) 1363.
- [11] P. Ahmad, A. Khalid, M.U. Khandaker, F. Rehman, M.I. Khan, H. Ali, N. Muhammad, M.S. Kiyani, A. Sulieman, M.A.R. Khan, The antibacterial and antioxidant efficacy and neutron sensing potency of 10B enriched hexagonal boron nitride nanoparticles, *Mater. Sci. Semicond. Process.* 141 (2022) 106419.
- [12] A. Khalid, P. Ahmad, S. Muhammad, A. Khan, M.U. Khandaker, M.M. Alam, M. Asim, I.U. Din, J. Iqbal, I.U. Rehman, Synthesis of boron-doped zinc oxide nanosheets by using phyllanthus emblica leaf extract: a sustainable environmental applications, *Front. Chem.* 10 (2022) 930620.
- [13] P.C. Ricci, C.M. Carbonaro, L. Stagi, M. Salis, A. Casu, S. Enzo, F.J.T.J.o.P.C.C. Delogu, Anatase-to-rutile phase transition in TiO<sub>2</sub> nanoparticles irradiated by visible light, *J. Phys. Chem. C* 117 (2013) 7850–7857.
- [14] B. Bharati, A. Sonkar, N. Singh, D. Dash, C. Rath, Enhanced photocatalytic degradation of dyes under sunlight using biocompatible TiO<sub>2</sub> nanoparticles, *J. Materials Research Express* 4 (2017) 085503.
- [15] A. Khalid, P. Ahmad, A.I. Alharthi, S. Muhammad, M.U. Khandaker, M.R. Iqbal Faruque, I.U. Din, M.A. Alotaibi, Unmodified titanium dioxide nanoparticles as a potential contrast agent in photon emission computed tomography, *Crystals* 11 (2021) 171.

- [16] Z. Razzaq, A. Khalid, P. Ahmad, M. Farooq, M.U. Khandaker, A. Sulieman, I.U. Rehman, S. Shakeel, A. Khan, Photocatalytic and antibacterial potency of titanium dioxide nanoparticles: a cost-effective and environmentally friendly media for treatment of air and wastewater, *Catalysts* 11 (2021) 709.
- [17] M. Hafeez, S. Afyaz, A. Khalid, P. Ahmad, M.U. Khandaker, M.U.K. Sahibzada, I. Ahmad, J. Khan, F.A. Alhumaydhi, T.B. Emran, Synthesis of cobalt and sulphur doped titanium dioxide photocatalysts for environmental applications, *J. King Saud Univ. Sci.* 34 (2022) 102028.
- [18] A. Khalid, P. Ahmad, A.I. Alharth, S. Muhammad, M.U. Khandaker, M.R.I. Faruque, I.U. Din, M.A. Alotaibi, A practical method for incorporation of Fe (III) in Titania matrix for photocatalytic applications, *Mater. Res. Express* 8 (2021) 045006.
- [19] A. Khalid, P. Ahmad, M. Uddin Khandaker, Y. Modafar, H.A. Almukhlifi, A.S. Bazaid, A. Aldarhami, A.M. Alanazi, O.A. Jefri, M.M. Uddin, Biologically reduced zinc oxide nanosheets using *Phyllanthus emblica* plant extract for antibacterial and dye degradation studies, *J. Chem.* (2023) 2023.
- [20] A. Khalid, Z. Razzaq, P. Ahmad, B.S. Al-Anzi, F. Rehman, S. Muhammad, M.U. Khandaker, G. Albasher, N. Alsultan, I. Liaqat, Visible-light promoted chemical fixation of carbon dioxide with epoxide into cyclic carbonates over S-scheme CdS–CeO<sub>2</sub> photocatalyst, *Mater. Sci. Semicond. Process.* 165 (2023) 107649.
- [21] Z. Rizwan, A. Zakaria, W.M.M. Yunus, M. Hashim, A.H. Shaari, Photopyroelectric spectrum of MnO<sub>2</sub> doped Bi<sub>2</sub>O<sub>3</sub>-TiO<sub>2</sub>-ZnO ceramic combination, *Pertanika Journal of Science & Technology* 16 (2008).
- [22] D. Achudhan, S. Vijayakumar, B. Malaikozhundan, M. Divya, M. Jothirajan, K. Subbian, Z.I. González-Sánchez, S. Mahboob, K.A. Al-Ghanim, B.J.J.o.E.C. E. Vaseeharan, The antibacterial, antibiofilm, antifogging and mosquitocidal activities of titanium dioxide (TiO<sub>2</sub>) nanoparticles green-synthesized using multiple plants extracts, *J. Environ. Chem. Eng.* 8 (2020) 104521.
- [23] B. Malaikozhundan, S. Vijayakumar, B. Vaseeharan, A.A. Jenifer, P. Chitra, N.M. Prabhu, E.J.M.p. Kannapiran, Two potential uses for silver nanoparticles coated with *Solanum nigrum* unripe fruit extract: biofilm inhibition and photodegradation of dye effluent, *Microb. Pathog.* 111 (2017) 316–324.
- [24] B. Malaikozhundan, R. Krishnamoorthi, J. Vinodhini, K.S.N. Nambi, S.J.I.C.C. Palanisamy, Multifunctional iron oxide nanoparticles using *Carica papaya* fruit extract as antibacterial, antioxidant and photocatalytic agent to remove industrial dyes, *Inorg. Chem. Commun.* 144 (2022) 109843.
- [25] B. Malaikozhundan, V.N. Lakshmi, R.J.M.T.C. Krishnamoorthi, Copper oxide nanoparticles using *Mentha spicata* leaves as antibacterial, antibiofilm, free radical scavenging agent and efficient photocatalyst to degrade methylene blue dyes, *Mater. Today Commun.* 33 (2022) 104348.
- [26] S. Ragupathy, S. Ramasundaram, G. Thennarasu, P. Harishenthil, M. Krishnakumar, T.H.J.C.I. Oh, Effect of Mn doping on structural, optical and photocatalytic properties of SnO<sub>2</sub> nanoparticles, *Ceram. Int.* 49 (2023) 17776–17783.
- [27] M. Ramamoorthi, D. Mani, M. Karunanithi, J.J. Mini, A. Babu, D. Mathivanan, S. Ragupathy, Y.-H.J.J.o.M.S. Ahn, Influence of metal doping and non-metal loading on photodegradation of methylene blue using SnO<sub>2</sub> nanoparticles, *J. Mol. Struct.* 1286 (2023) 135564.
- [28] A.M. Shahat, F. El-Hossary, A. Ghitas, A. Abd El-Rahman, A. Ebnalwaled, Low-temperature hydrothermal synthesis of titanium dioxide nanoparticles for photocatalytic applications, in: *IOP Conference Series: Materials Science and Engineering*, IOP Publishing, 2021 012008.
- [29] K. Umar, A. Aris, H. Ahmad, T. Parveen, J. Jaafar, Z.A. Majid, A.V.B. Reddy, J. Talib, Synthesis of visible light active doped TiO<sub>2</sub> for the degradation of organic pollutants—methylene blue and glyphosate, *Journal of Analytical Science and Technology* 7 (2016) 29.
- [30] A.A. Torrano, Á.S. Pereira, O.N. Oliveira Jr., A. Barros-Timmons, Probing the interaction of oppositely charged gold nanoparticles with DPPG and DPPC Langmuir monolayers as cell membrane models, *Colloids Surf. B Biointerfaces* 108 (2013) 120–126.
- [31] J. Bi, X. Cao, Electrochemical Properties and thin-film morphology of Mn-doped TiO<sub>2</sub> thin layer prepared by electrodeposition technique and its application as photocatalyst for Rhodamine B degradation, *Int. J. Electrochem. Sci.* 16 (2021).
- [32] P. Praveen, G. Viruthagiri, S. Mugundan, N. Shanmugam, Sol-gel synthesis and characterization of pure and manganese doped TiO<sub>2</sub> nanoparticles—A new NLO active material, *Spectrochim. Acta Mol. Biomol. Spectrosc.* 120 (2014) 548–557.
- [33] J.A. Dias, A.L. Freire, I. Girotto, C. Del Roveri, V.R. Mastelaro, E.C. Paris, T.R. Giraldi, Phase evolution and optical properties of nanometric Mn-doped TiO<sub>2</sub> pigments, *Mater. Today Commun.* 27 (2021) 102295.
- [34] L. Wan, Y. Gao, X.-H. Xia, Q.-R. Deng, G. Shao, Phase selection and visible light photo-catalytic activity of Fe-doped TiO<sub>2</sub> prepared by the hydrothermal method, *Mater. Res. Bull.* 46 (2011) 442–446.
- [35] S.R. Muditana, S.R. Tirukkavalluri, I.M. Raju, Synthesis and antibacterial activity of transition metal (Ni/mn) CO-doped TiO<sub>2</sub> nanophotocatalyst on different pathogens under visible light irradiation, *Наносистемы: физика, химия, Математика* 13 (2022) 104–114.
- [36] M. Zahid, E.L. Papadopoulou, G. Suarato, V.D. Binas, G. Kiriakidis, I. Gounaki, O. Moira, D. Venieri, I.S. Bayer, A. Athanassiou, Fabrication of visible light-induced antibacterial and self-cleaning cotton fabrics using manganese doped TiO<sub>2</sub> nanoparticles, *ACS Appl. Bio Mater.* 1 (2018) 1154–1164.
- [37] P.R. Ettireddy, N. Ettireddy, S. Mamedov, P. Boolchand, P.G. Smirniotis, Surface characterization studies of TiO<sub>2</sub> supported manganese oxide catalysts for low temperature SCR of NO with NH<sub>3</sub>, *Appl. Catal. B Environ.* 76 (2007) 123–134.
- [38] Z. Mo, N.I.F. Aktivnostjo, Hydrothermal synthesis of Mn-doped TiO<sub>2</sub> with a strongly suppressed photocatalytic activity, *Materiali in tehnologije* 52 (2018) 411–416.
- [39] S.M. Al-Jawad, M.M. Ismail, S.F. Ghazi, Characteristics of diluted magnetic semiconductor based on Mn-doped TiO<sub>2</sub> nanorod array films, *J. Solid State Electrochem.* 25 (2021) 435–443.